Engineering Research Journal
journal homepage: https://erj.journals.ekb.eg/

Keys Investigation on the Performance of Wide Beam Column Joints Under Static Loading, an Analytical Study

Toka R. Mohamed [1,*], Mohamed H. Agamy [1] and Nehal M. Ayash [1]

[1] Civil Engineering Department, Faculty of Engineering at Mataria, Helwan University, Cairo 11718, Egypt.

*Corresponding author E-mail: tokarefaat296@m-eng.helwan.edu.eg

Abstract. In many cases, beam's width is larger than column width which is named wide or shallow beam joint. This joint type has architectural and structural benefits. But the transmission of bending moments from wide beams to the columns was not sufficient and the energy dissipation capacity of this joint was low. The behavior of wide beam column joint is needed extremely study under various conditions. Numerical study is necessary to supplement the experimental method and can explore effects of different parameters with less time, apparatus and cost than experimental tests. The current study is conducted on exterior beam column joints. The studied parameter is beam to column width ratio compared to conventional joints with the same beam width. Firstly, 3D finite element models using "ANSYS" were developed to validate analytical models in capturing the pervious experimental study. Then more numerical models are constructed to evaluate the effect of different parameters. Also, the theoretical calculations depending on ACI318-19 international code provisions are compared with numerical analysis.

The results demonstrate that increasing beam width leads to higher strength but reduces ductility for higher beam to column width ratio while conventional beam-column joints exhibited higher strength and stiffness compared to wide beam-column joints. The study also highlights the limitations of ACI 318-19 predictions regarding joint shear capacity, suggesting potential modifications for more accurate design provisions. Overall, the findings provide insights into optimizing wide beam-column joint designs for better performance.

Keywords: Wide Beam, Beam Column Joint; Finite Element; Joint Shear Stress, ACI 318-19

1. Introduction

Reinforced concrete moment resisting frames with wide beam-column joint are commonly used for over many decades as a structural system of concrete building due to its numerous benefits, including increasing floor clear height, which lowers the overall building height, simplified formwork requirements that reduce construction cost and time, reduced need for shear links due to higher beam

DOI: 10.21608/erj.2025.375297.1227
Received 02 May 2025; Received in revised form 02 May 2025; Accepted 11 July 2025
Available online 01 September 2025

width and longer spans compared to flat slab system. Nowadays, the use of this structural system has been steadily increasing because of the mentioned advantages.

It has been noted that behavior of frames and its failure mode depends on beam column joint and its proper design and detailing, so several design methods and many studies have been developed for studying the behavior of beam column joints under different loads. Obviously, wide beam column joints behavior differs than conventional beam column joints because of portion of beam longitudinal reinforcement not anchored to column core that may increase joint shear and cause torsional moments in joint region. Their behavior was investigated previously in much past research**.**

S.S. Mahini and H.R. Ronagh (2007) [1] tested plain and CFRP-retrofitted beam column joints of under monotonic and cyclic loads to failure. The CFRP-retrofitting technique effectively relocates the plastic hinging zone away from the column face, enhances beam strength to maintain elasticity near the column, and reduces shear deformation with transverse wraps, achieving inelastic deformations around 150 mm from the column as expected. A.M. Elsouri and M.H. Harajli (2013) [2] reported a two-part experimental investigation of the seismic behavior of exterior wide beam-narrow column connections constructed in the Middle East. In the first part, two full-scale gravity-load designed (as-built) joints were tested under quasi-static cyclic loads, failing prematurely due to joint shear failure at low drift ratios (1.0-1.5%), showing poor seismic resistance. In the second part, two earthquake-resistant joints with improved reinforcement were tested. These joints showed better seismic performance, with higher lateral load capacity, deformation, energy dissipation, and a stable hysteretic response. S. Mirzabagheri and A.A. Tasnimi (2016) [3]. conducted an experimental test comparing between wide and conventional roof exterior beam–column joints. Tests revealed that the exterior wide beam–column joint exhibited greater ductility compared to exterior conventional joint. However, there was no significant difference in strength or energy dissipation capacity between the two specimens. Additionally, the joint shear strength in the wide beam–column joint was found to be sufficient. H. Behnam, et al. (2016) [4] presented experiments on two full-scale wide beam-column connections, differing only in spandrel beam reinforcement. The control specimen, with reinforcement, showed ductile failure via beam flexural hinging followed by joint and torsional failure. The other specimen, lacking reinforcement, experienced brittle torsional failure and a 37% reduction in flexural strength. Nonlinear finite element analysis was also conducted, confirming that controlling joint shear and torsional stresses is essential for ensuring adequate seismic performance in wide beam-column connections. H. Behnam, et al. (2017) [5] investigated experimentally the impact of the beam width to column width ratio on the seismic behavior of exterior beam-column connections. Four specimens, designed according to ACI 318-14 and ACI 352R-02, were tested under reversed cyclic loading. The beam width ratios ranged from 1 to 2.5, with joint shear stress ratios from 0.74 to 2.03. Specimens with beam width ratios of 1 and 1.5 showed good seismic performance, allowing full beam plastic hinge formation without significant joint damage. However, specimens with higher beam width ratios experienced significant joint core damage. Also, spandrel beam torsional failure was observed in specimen with beam width ratio of 2.5. H. Behnam, et al. (2018) [6] conducted a numerical study using ABAQUS to investigate the effects of column axial load, column and beam dimensions, beam bar anchorage ratio, and spandrel beam reinforcement on the performance of exterior wide beam-column connections. Studies proved increasing column width and depth improves the seismic performance of wide beam-column connections. Enhancing beam depth while reducing longitudinal reinforcement also benefits the response by strengthening the spandrel beam and reducing torsion and joint shear stress. H. Behnam, et al. (2018) [7] developed an effective beam-width model for exterior wide beam–column connections using an equivalent-frame model, considering torsion of transverse beams and flexure around the joint core. A formula is proposed to determine the beam-width limitation, aimed at minimizing shear lag, ensuring proper yielding of beam longitudinal bars and avoiding torsional cracking of transverse beams. The studies recommended limiting the beam width to $b_w \leq (b_c+\beta h_c)$ where β varies from 0.6 to 1.5 depending on the beam and column dimensions. H. Behnam, et al. (2018) [8] conducted an experimental study on two full-scale exterior wide beam–column connections tested under lateral quasi-static cyclic loading. The control

specimen had both longitudinal and transverse spandrel beam reinforcement, while the second specimen used post-tensioning. The control specimen reached its flexural capacity at 3% drift but suffered joint shear and torsional failure. In contrast, the post-tensioned specimen showed improved seismic performance, sustaining 5% drift with no significant strength loss or failure. Post-tensioning enhanced joint shear capacity and displacement ductility, preventing torsional failure. R.P. Bohara, et al. (2019) [9] showed force–displacement hysteresis behavior and failure pattern of full-scale post-tensioned precast wide U beam–column interior joint due to displacement-controlled lateral cyclic load. X. Gao, et al. (2020) [10] tested five full-scale RC exterior joints to measure deformations, reinforcement strains, and hysteretic behavior, while analyzing crack patterns and failure modes. Results showed shear deformation in the joint core, influenced by beam depth and stirrup volume, was significant in the plastic stage. V. V S and N. Mohan (2020) [11] studied literature on exterior wide beam-column connections under seismic loading. Researchers highlighted the critical influence of geometric discontinuities and spandrel beam torsional behavior on overall seismic performance, including ultimate strength, stiffness, and energy dissipation. A. Pakzad and M. Khanmohammadi (2020) [12] investigated the seismic behavior of exterior wide connections under axial and cyclic lateral loads. Specimens varied in spandrel beam types (conventional and wide) and column geometries (square, rectangular, and circular). Results showed satisfactory performance in strength, ductility, and energy dissipation, with more torsional cracks in specimens with wide transverse beams. Circular columns exhibited higher ductility but lower energy dissipation than square columns. The study emphasized the critical role of precise reinforcement detailing in the joint zone. R.Y.C. Huang and J.S. Kuang (2020) [13] developed an analytical model to estimate the strength of reinforced concrete wide beam-column joints. The model combined the softened strut-and-tie approach for the joint core and a thin-walled tube space truss analogy for the outer joint. The model's strength predictions were validated against 30 experimental results and compared with the predictions from three major seismic design codes. R.P. Bohara, et al. (2021) [14] presented an experimental and analytical investigation for studying the behavior of a half-scale post-tensioned precast wide U beam-column interior joint under incremental lateral cyclic loading. Results showed that the precast joint had equivalent load-displacement behavior to a monolithic joint with similar detailing. J.H. Kim, et al. (2023) [15] conducted experimental and numerical studies on wide joints to evaluate load-drift relationships, failure modes, and seismic performance. The results showed that increasing the ratio of outer to inner longitudinal reinforcement bars causes more severe concrete damage, reducing their seismic performance. Q. Jiang, et al. (2024) [16] examined the seismic performance of wide exterior beam-column joints using seven half-scale specimens. Results show bending damage at beam ends, strong column–weak beam behavior, and reduced ductility with increased beam width and concrete strength. Axial load improves joint strength for narrow beams, but bond-slip issues arise with longitudinal bars outside the column core.

Because of the significant effect of beam-column joints on the structural system, design codes place special requirements for joint design. In ACI 318-19 and ACI 352R-02, for conventional and wide beam-column connections, key design parameters ensure flexural hinging occurs in beams rather than columns, with a column-to-beam flexural strength ratio of at least 1.2. Joint shear must not exceed the nominal strength to prevent failure before beam hinging, and transverse reinforcement is required to control joint deterioration during seismic events. ACI 318-19 and ACI 352R-02 have more requirements for wide beam-column connections than conventional ones, including limiting beam width not to exceed the lesser of (b_c+1.5h_c) and (3b_c), with at least 1/3 of the top beam reinforcement anchored inside the column core. Additionally, spandrel beams should be designed to resist torsional forces from anchored beams and slab bars.

The existing data from the literature review focuses on the effects of beam-to-column width ratio, joint shear stress, and spandrel beam dimensions, but reveals a lack of studies on eccentric beam-column joints or the impact of different compressive strengths between the column and beam.

2. Research Significant

The current study presents an analytical verification against previous experimental data on the behavior of wide and conventional beam column joints using the finite element software ANSYS. The study will investigate the influence of beam width on the behavior of conventional beam column joints. For wide joints, the parameter studied is change of beam to column width ratio for exterior joints. Results will be calibrated with predictions obtained from different international design codes.

3. Verification study

In this section, a verification study is conducted on a pervious experimental study for calibration of finite element model of beam column joint.

3.1 Description Specimens by S.S. Mahini And H.R. Ronagh(2007)

External beam column joint from 1/2.2 scaled frame was tested by S.S. Mahini and H.R. Ronagh (2007) [17]. The specimen consists of a beam having dimensions180mm x 230mm reinforced with 4Ø12 as longitudinal bars. The column section is 220mm x180mm reinforced with 4Ø12. Both beam and column have stirrups of R6.5 bars at spacing of 150mm. Longitudinal reinforcement and stirrups have yield strengths of 500 Mpa and 382 Mpa, respectively. Control specimen (CSM0) has a compressive strength of concrete around 40 MPa and modulus of elasticity around 27.6 GPa. A 30 mm clear cover for both beam and column is used. Additional stirrups and N16 threaded rods were placed near the ends of the beam and column; as shown in (Fig. 1); to ensure that local failure does not occur at the load and support points.

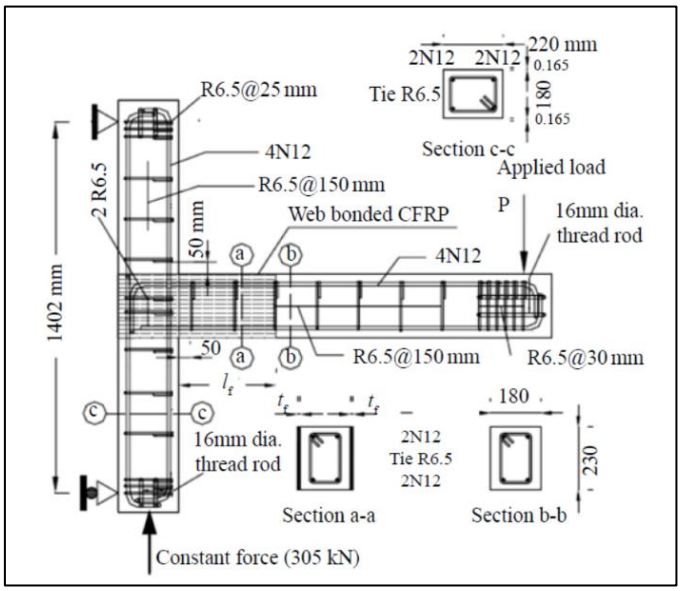

Fig. 1. Beam-column joint by Mahini and Ronagh, 2007 [17]

Specimen was supported by hinged supports at column ends that allow rotation, but do not allow translation. The column was loaded axially by constant load (305 kN) during test while an incremental static load was applied on beam end until failure.

3.2 Description of the numerical model.

Joint was modeled using ANSYS, 2019 software as shown in (Fig. 2) to compare results with experimental tests.

3.2.1. Modeling.

Solid 65 -an eight-node element- is used to model concrete. 3D line elements (Link 180) are used for modeling of reinforcement bars. Steel plates at beam supports and load plates are modeled as solid 185 elements.

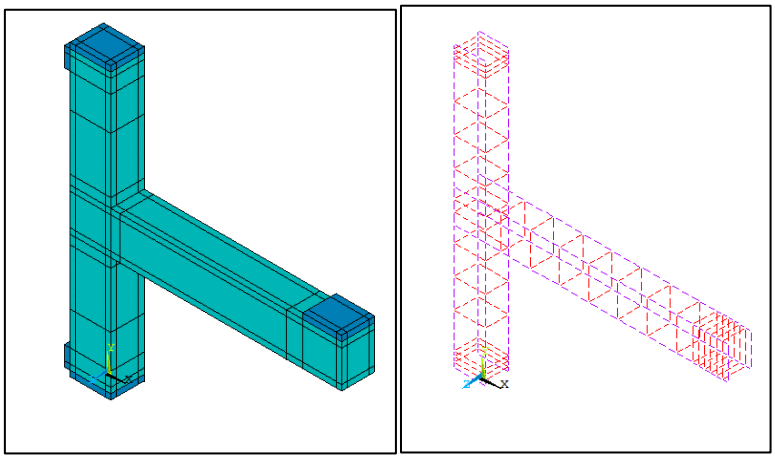

Fig. 2. Geometry of control specimen ANSYS model.

3.2.2. Properties of material.

Table 1 shows material properties of concrete. Linear isotropic properties as modules of elasticity and Poisson's ratio. The nonlinear properties of concrete are defined as "Concrete" property by defining cracking and crushing strengths and open/closed shear transfer coefficients for cracking. The tensile strength has been calculated as f_{ctr}=0.6$\sqrt{f_{cu}}$. The open shear transfer coefficient is best set between 0.1 and 0.3 to simulate minimal shear in open cracks, while the closed shear transfer coefficient should range from 0.7 to 1.0 to reflect higher shear capacity in closed cracks due to aggregate interlock. These values help achieve realistic concrete shear behavior under load. In this study, the open and closed shear transfer coefficients are taken to be 0.3 and 0.9, respectively. Multilinear Isotropic Hardening property is assigned to define the stress-strain relationships of concrete up to crushing.

Table 1. Material properties of concrete

Material Properties of Concrete for Solid65		
Linear Isotropic		
EX	29703 Mpa	
PRXY	0.2	
Multilinear Isotropic		
Point	Strain (mm)	Stress (Mpa)
1	0.000404	12
2	0.0006	16.99
3	0.0009	24.06
4	0.0012	29.75
5	0.0015	34.02
6	0.0018	36.97
7	0.002691	40
8	0.003	40
Concrete		

Open Shear Transfer Coef	0.3
Closed Shear Transfer Coef	0.9
Uniaxial Cracking Stress	4.42 Mpa
Uniaxial Crushing Stress	40 Mpa

The material properties of steel reinforcement are listed in *Table 2*. The "Linear Isotropic" property is used to define the modules of elasticity and Poisson's ratio, whereas the "Bilinear Isotropic" characteristic is used to describe yield stress and the tangent modulus.

Table 2. Material properties of steel used in FE models

Property	Ø 12, Ø 16	Ø 6.5
Yield Stress (MPa)	500	382
Tangent Modulus (MPa)	2000	
Modulus of Elasticity E (MPa)	200000	
Poisson's Ratio ν	0.3	

3.2.3. Meshing, Boundary condition and loading

To improve the accuracy, three different mesh sizes were explored. Based on the experimental failure load that is occured at 24.64 KN, the models with mesh sizes as 25 mm, 50 mm, and 75 mm failed at 20.4 kN (82.8%), 24 kN (97%), and 23.1 kN (93.6%), respectively. These findings led to the selection of a mesh size taken as 50 mm.

After defining the geometry of model, material properties and mesh size, boundary condition and loading need to be defined. The displacement boundary condition was defined to constrain the model. Column has top vertical supporting plate with the same column area that restrains Ux, Uy and Uz, top lateral support restrains Ux, Uy and Uz for 0.1 of column height approximately and bottom lateral one restrains Ux only. Constant concentrated load (305 kN as per experimental test) was applied axially on loading plate at the bottom of column. An incremental load was applied as a concentrated load at loading plate with dimension 210mm x180mm on beam end in – y direction. Load increased by 2 kN for each load step until failure and the results of each load increment have been recorded. (Fig. 3) shows meshing and loading set up of beam and column.

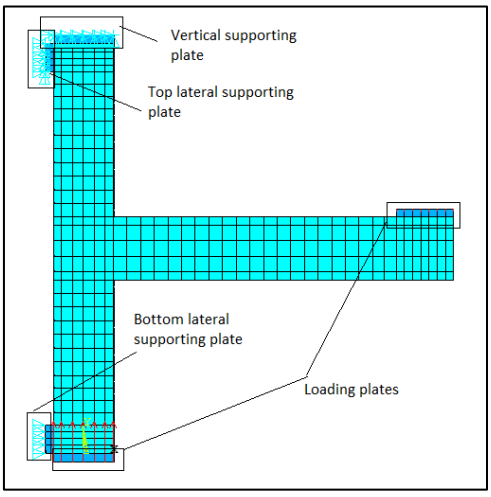

Fig. 3. Meshing and loading of control specimen ANSYS model.

3.2.4. Analysis type.

The type of static analysis is carried out. The Full Newton-Raphson approach is used to adopt the nonlinear equations, and there are enough sub-steps in the loading process to capture all the behavior's stages, such as yielding, failure, and cracking. For concrete issues, a 5% convergence tolerance is assumed depending on the displacement degree of freedom. Loading is carried out on two load steps; the column is loaded constantly at first load step while the beam is loaded gradually during the second load step. To limit the constant load sub-step, the automated time stepping is set to OFF. Common instructions used in a static analysis that is nonlinear are displayed in *Table 3.*

Table 3. Commands Used to Control Nonlinear Analysis

Load step	First load step	Second load step
Analysis options	Small displacement static	Small displacement static
Calculate prestress effects	No	No
Time at end of load step	1	30000
Automatic time stepping	Off	Off
Number of sub steps	1	50
Min Number of sub steps	1	50
Max Number of sub steps	1	100
Frequency	Write every sub step	Write every sub step
Write items to result file	All solution items	All solution items

3.2.5. Validation results.

Comparison was concerned on failure load and failure pattern of specimen Failure occurred at monotonic load around 24.64 KN in the experimental test while the analytical model failed at 24 KN that means analytical solution reaches accuracy of 97 % of experimental results. Also, the behavior of beam column joint in the analysis is close to the experimental tests as shown in crack pattern in (Fig. 4) where failure occurred due to propagation of flexural cracks near to column face. Top longitudinal beam reinforcement bars reached their maximum yield stress at column face which is the same as mentioned in experimental results.

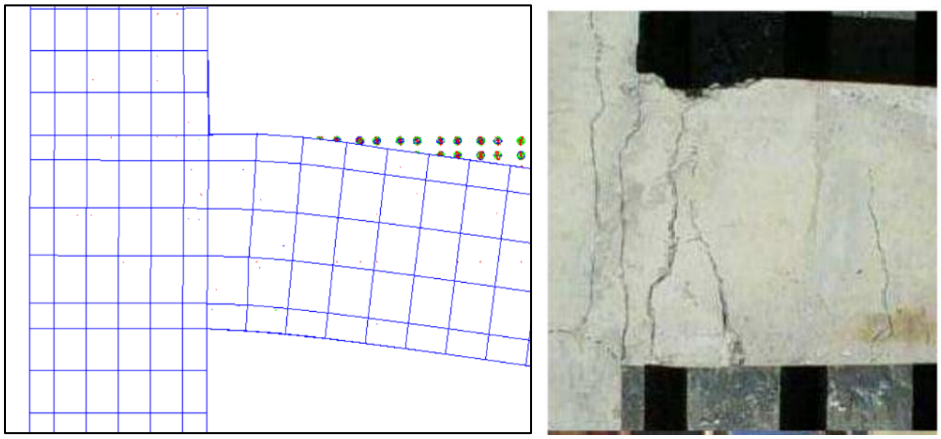

Fig. 4. Close up of cracking behavior of the control specimen (Experimental by Mahini and Ronagh, 2007 versus analytical by Ansys).

4. Parametric study

Wide beam column joint finite element models were built with various parameters. To compare the exterior beam column connection with the comparable conventional beam column joint, which has the same beam width and beam to column width ratio equal to 1, this study examines the effects of the beam to column width ratio varied by 1, 1.5, 2, and 2.5.

4.1 Description of the numerical model

Seven specimens of exterior beam column joints are conducted to cover the study as listed in Table 4. (Fig. 5) shows details and dimensions of exterior beam column joints. All specimens consist of a beam 1500 mm length from column face and a column with height 3300 mm. All beams are 300 mm depth, and all columns are 450 mm depth. Beams and columns widths and longitudinal reinforcement are varied for different specimens. Both beam and column have stirrups of (Ø10 mm) bars at spacing of 150mm. Columns stirrups are extended through the joint. Conventional beam column joints have beam framing in one direction while wide joints have wide beam framing in the main direction and spandrel beam in the transverse direction.

For wide beams, only four bars of beam longitudinal reinforcement are anchored to column core while other bars are anchored to spandrel beam. Spandrel beam has the same depth as beam and its width is similar to column depth with 5Ø12 mm top and bottom longitudinal reinforcement and closed hoops of (Ø10 mm) spaced by 70 mm.

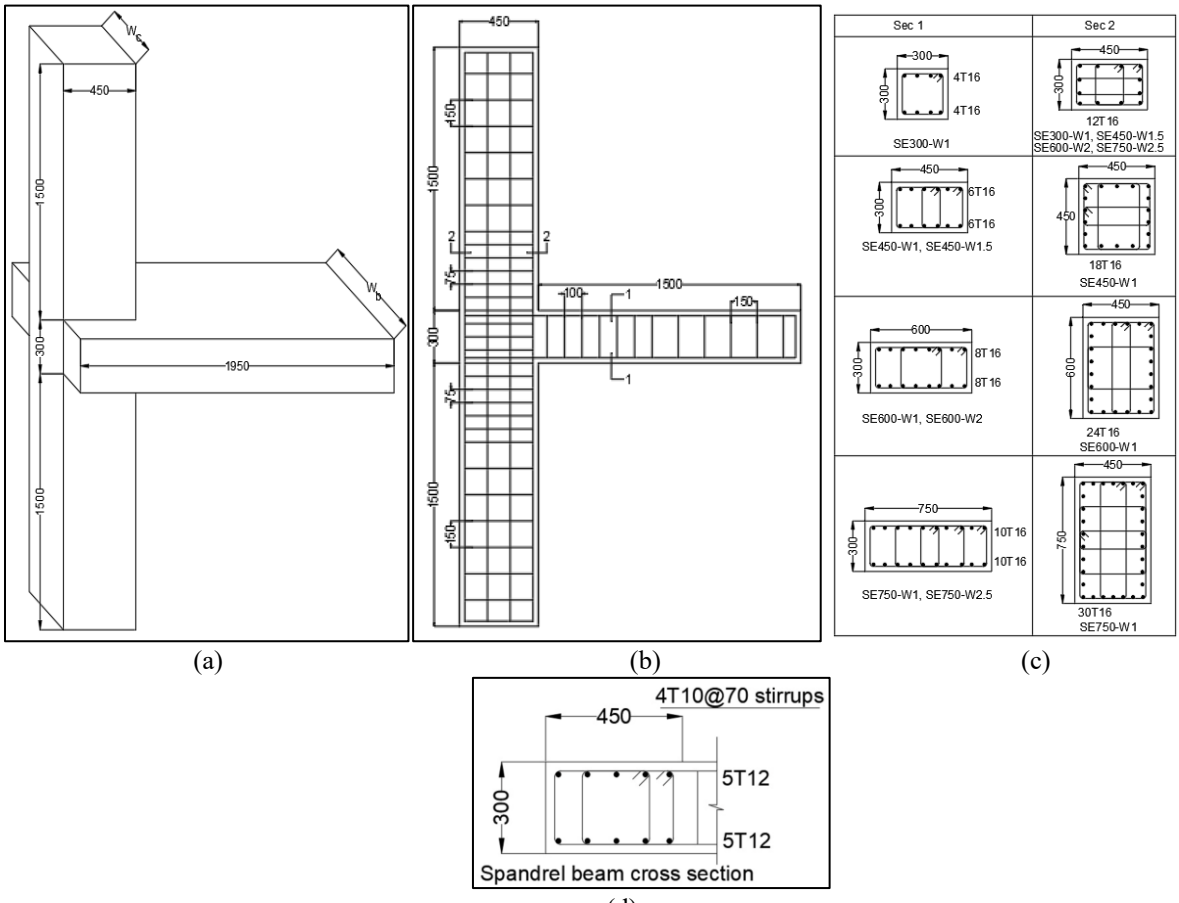

Fig. 5. Concrete dimension and reinforcement of (a) 3-D view, (b) Sectional elevation, (c) Cross sections of column and beam, and (d) Spandrel beam

Table 4. Models' geometry and reinforcement used in parametric study

Specimens	Beam			Column			Spandrel beam		
	Dimensions (300* W_b) (mm)	Long. Reinf.	Stirrups	Dimensions (450*W_c) (mm)	Long. Reinf.	Stirrups	Dimensions (mm) @ both sides	Long. Reinf.	Stirrups
SE300-W1.0	300*300	4Ø16	Ø10 bars @ 150 mm	450*300	12Ø16	Ø10 bars @ 150 mm	------	------	Ø10 closed hoops @ 70 mm
SE450-W1.0	300*450	6Ø16		450*450	16Ø16		------	------	
SE600-W1.0	300*600	8Ø16		450*600	24Ø16		------	------	
SE750-W1.0	300*750	10Ø16		450*750	30Ø16		------	------	
SE450-W1.5	300*450	6Ø16		450*300	12Ø16		75	5Ø12	
SE600-W2.0	300*600	8Ø16		450*300	12Ø16		150	5Ø12	
SE750-W2.5	300*750	10Ø16		450*300	12Ø16		225	5Ø12	

The naming convention for the specimens is structured to provide clear identification of key parameters. The letter "S" represents the term specimen, while "E" indicates an exterior joint, with the number following "E" denoting the beam width. The letter "W" followed by a number specifies the beam-to-column width ratio.

Modeling. Simulations of element types are conducted in accordance with analysis procedure and details discussed in validation modeling details. (Fig. 6) shows details of exterior wide beam column joint- ANSYS model (a) Geometry and (b) Reinforcement.

Properties of material. As discussed, both linear and nonlinear properties are necessary to define the concrete material. *Table 5* provides these properties for concrete. All joints have a concrete compressive strength of approximately 30 MPa and a modulus of elasticity around 25.7 Gpa. Linear and bilinear properties of reinforcement used in FE models are shown in

Table **6**. longitudinal bars and stirrups have modulus of elasticity equal to 200 GPa and the yield strenghs is 500 MP for longitudinal bars and420 Mpa for stirrups.

Meshing, Boundary condition and loading. (Fig. 7) shows the geometry and meshing of a specimen model for exterior joints with mesh size 50 mm based on validation model.

Table 5. Material properties of concrete

Material Properties of Concrete for Solid65		
EX	25714 Mpa	
PRXY	0.2	
Point	Strain (mm)	Stress (Mpa)
1	0.00035	9
2	0.0006	14.49
3	0.0009	20.16
4	0.0012	24.42
5	0.0015	27.31
6	0.0018	29.03
7	0.002331	30
8	0.003	30
Open Shear Transfer Coef		0.3
Closed Shear Transfer Coef		0.9
Uniaxial Cracking Stress		3.67 Mpa
Uniaxial Crushing Stress		30 Mpa

Table 6. Material properties of steel used in FE models

Property	Ø 12, Ø 16	Ø 10
Yield Stress (MPa)	500	420
Tangent Modulus (MPa)	2000	2000
Modulus of Elasticity E (MPa)	200000	200000
Poisson's Ratio ν	0.3	0.3

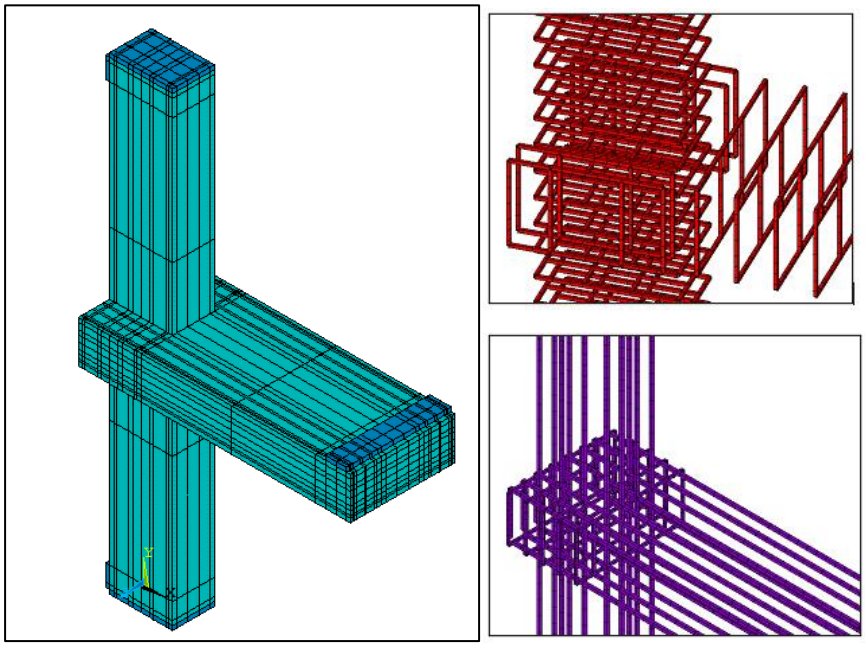

(a) (b)

Fig. 6. Details of exterior wide beam column joint- ANSYS model (a) Geometry and (b) Reinforcement.

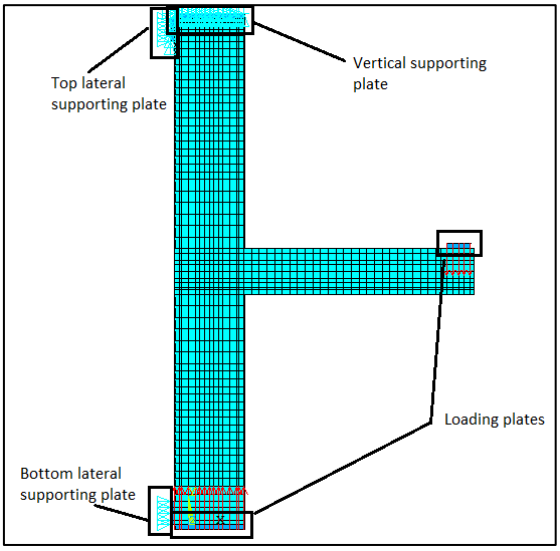

Fig. 7. Meshing and loading of control specimen ANSYS model.

The displacement boundary condition was defined to constrain the model for both exterior and interior joint are conducted as va;idation model. Constant concentrated load (500 kN that represents 25% of column axial capacity) was applied axially on loading plate with the same area of column section at the bottom of column. During applying the constant load, external joints are loaded with incremental concentrated load at loading points of loading plate with the same width of the beam and 150mm length

on beam top in – y direction. Load increased by 2 kN for each load step until failure and the results of each load increment have been recorded. (Fig. 7) shows loading set up of beam and column.

4.2 Expected capacities

Table 7 summarizes the expected capacities of specimens calculated depending on ACI318-19 [18] and ACI352-02r [19] provisions and compares them with the numerical results. Beam vertical load capacity ($V_{b,ACI}$) is calculated using nominal beam flexural strength ($M_{n,b,ACI}$) where ($V_{b,ACI} = M_{n,b,ACI}/L_b$) and L_b is beam length. Nominal flexural strength ($M_{n,b,ACI}$), nominal torsional moment (T_n) and concrete cracking torsional moment (T_{cr}) are in accordance with ACI318-19 as follows:

$$M_{n,b,ACI}=f_y*A_s(d-a/2) \quad (1)$$

$$a=(f_y*A_s)/(0.85*f_{c'}*b_w) \quad (2)$$

$$T_{cr}=0.33\,\lambda\sqrt{f_{c'}}*(A_{cp}^2/P_{cp}) \quad (3)$$

$$T_n=2A_oA_tf_y\cot\theta/s \quad (4)$$

Where: f_y: yield stress of steel, A_S: area of beam longitudinal reinforcement, d: effective beam depth, $f_{c'}$: concrete compressive strength, b_w is beam width, λ shall be taken as 1.0 for normal weight concrete, A_{cp} represents cross section area confined by outside perimeter (P_{cp}), $A_o=0.85A_{oh}$ in which A_{oh} represents area confined by outer beam stirrup, A_t is the area of one leg of a closed stirrup resisting torsion and s is the longitudinal spacing between stirrups. Angle θ shall not be taken less than 30° or greater than 60° and it is permitted to be taken equal to 45° for no prestressed members.

Factored torsional moment ($T_{u,ACI}$) is calculated as ratio of nominal beam moment equal to the ratio of beam longitudinal rebars anchored outside column core to the total beam rebars.

Expected joint shear force (V_{JjACI}) is calculated in terms of reinforcement tension and column shear force (V_{col}) as follows:

$$V_{JjAC}=1.25\,f_y*A_s-V_{col} \quad (5)$$

Joint shear force should not exceed ϕV_n where ϕ is 0.75 for shear and nominal joint shear force (V_n) is calculated using joint area in accordance with ACI318-19:

$$V_n=1.3\,\lambda\,\sqrt{f_{c'}}\,b_c\,h_c \quad (6)$$

Where: b_c and h_c represent column horizontal section dimensions.

Table 7. Design parameters and expected capacities for exterior beam column joints.

Specimen	Expected capacities (ACI)						Analytical results			Analytical/expected				Failure Mode	
	Vb	Vj	$\frac{Vj}{\phi Vn}$	Tu	$\frac{Tu}{Tn}$	$\frac{Tu}{Tcr}$	Vb	Vj	Tu	$\frac{Vb_{ana}}{Vb_{ACI}}$	$\frac{Vj_{ana}}{\phi Vn}$	$\frac{Vj_{ana}}{Vk_{ACI}}$	$\frac{Tu_{ana}}{Tn_{ACI}}$	Exp.	Ana.
SE300-W1.0	70.22	462.90	0.64	0	0	0	76.0	360.37	0	1.08	0.50	0.78	0	F	F
SE450-W1.0	105.33	694.35	0.64	0	0	0	113.0	536.94	0	1.07	0.50	0.77	0	F	F
SE600-W1.0	140.44	925.80	0.64	0	0	0	153.0	718.74	0	1.09	0.50	0.78	0	F	F
SE750-W1.0	175.56	1157.25	0.64	0	0	0	192.0	896.92	0	1.09	0.50	0.78	0	F	F

SE450-W1.5	105.33	694.35	0.96	30.61	0.36	1.39	115.0	538.14	25.03	1.09	0.75	0.78	0.29	F	F
SE600-W2.0	140.44	925.80	1.28	61.23	0.72	2.79	151.0	718.92	49.76	1.08	1.00	0.78	0.58	S	F
SE750-W2.5	175.56	1157.25	1.61	91.84	1.08	4.18	159.0	808.37	63.48	0.91	1.12	0.70	0.74	S+T	S

Where: F = "Flexure" Failure Mode; S+T = "Joint shear & torsion" Failure Mode; and S = "Joint shear" Failure Mode

4.3 Effect of beam to column width ratio

Cracking pattern and failure mode. (Fig. 8) shows crack pattern at ultimate load for conventional beam and wide beam to column joints. The crack patterns reveal two primary types: vertical cracks, which indicate flexural failure, and diagonal cracks, which signify shear failure. For all conventional joints, flexure cracks appear first at beam near to column face then minor shear cracks begin to develop within the joint region. The ultimate failure of these conventional joints occurred when the applied load exceeded the beam's flexural capacity, indicating that flexure was the dominant failure mode.

Specimen SE450-W1.5 exhibited behavior similar to conventional joints. The major cracks in this specimen were due to flexure while shear cracks were only minor in joint region.

For specimens with higher beam to column width ratio such as SE60-W2.0 and SE750-W2.5, shear cracks became more obvious. The increase in shear cracking is expected to be due to joint shear force in additional to torsional moment of spandrel beam resulting from rebars not anchored to column core as shown in (Fig. 8).

Specimen SE600-W2.0 failed primarily due to flexure, but it also cracked due to shear significantly in the joint region. In contrast, specimen SE750-W2.5 failed due to propagation of shear cracks which developed and grew to critical levels before the load could reach the beam's flexural capacity. This indicates a shift in the failure mechanism, with shear forces overtaking flexure as the primary cause of failure in joints with very high beam-to-column width ratios.

For conventional joints and wide joints with beam to column width ratio of 1.5, it was expected to fail due to flexure depending on ACI 318-19 predictions that agreed with numerical results as shown in *Table 7*. While ACI 318-19 expected joints, with a ratio of 2 to fail due to joint failure but numerical results show they reached its full flexure capacity before failure. Also, the results of wide joint with a ratio of 2.5 complied with ACI 318-19 predictions as it failed due to joint shear and torsional moment of spandrel beam.

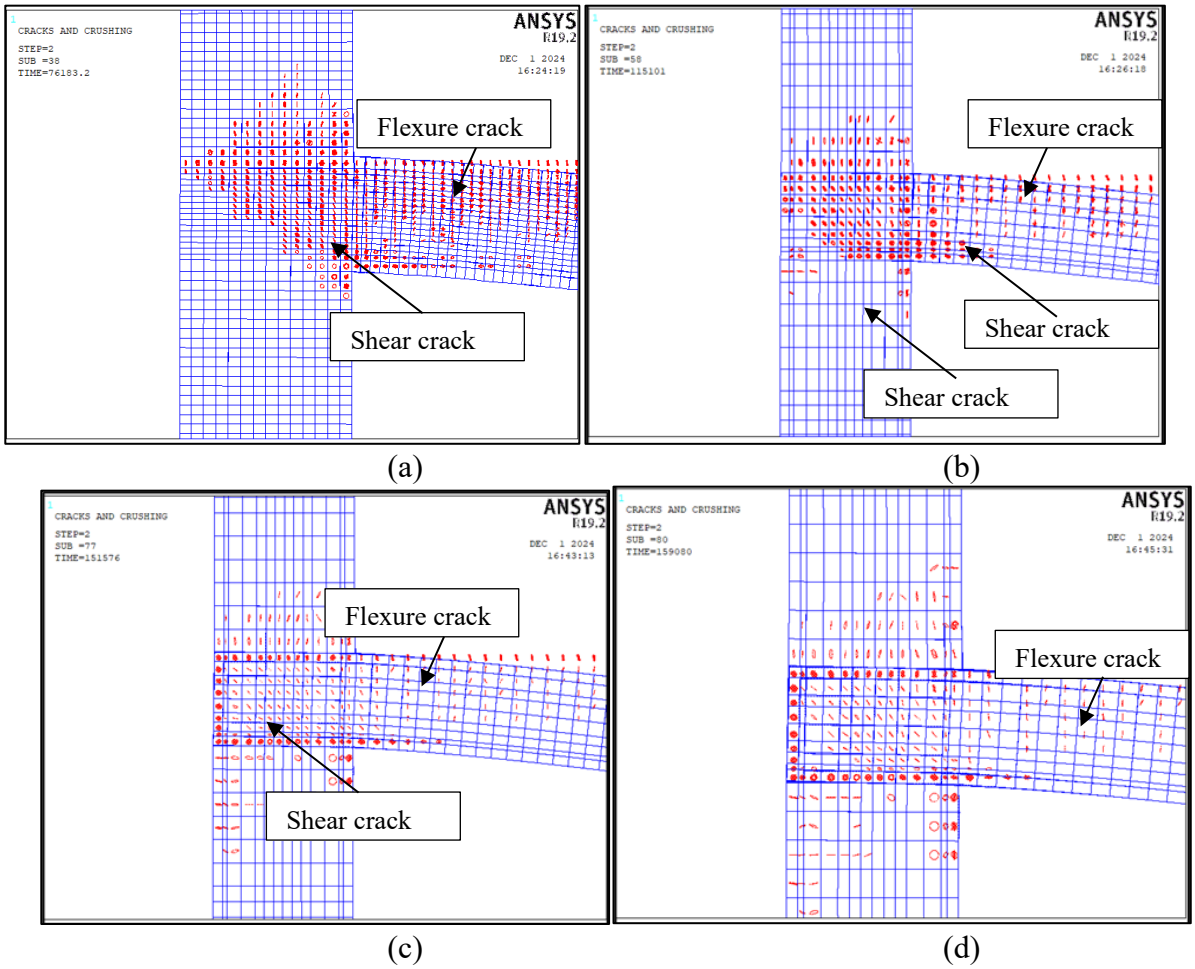

Fig. 8. Crack pattern at failure load for (a) SE300-W1.0 (b) SE450-W1.5 (c) SE600-W2.0 (d) SE750-W2.5.

Load displacement curve. (Fig. 9) represents the relation between the load and beam tip displacement. While *Table 8* shows values of load and displacement at first crack and ultimate case for wide and conventional joints obtained from load displacement curve. It shows comparison between conventional joints (beam width = column width) and wide joints (beam wider than column) using different beam widths (300, 450, 600, and 750 mm).

It has been noted that joint capacity is increased due to beam width increase for both conventional and wide joints cases. Conventional joints failed at strength equal to 76.18, 113.68, 153.94 and 192.19 kN for beam widths of 300, 450, 600 and 750mm respectively. The strength increases correspond closely to the ratios of beam width increases compared to SE300-W1, with strength ratios of 1.54, 2.02, and 2.52 aligning with the width ratios of 1.5, 2.0, and 2.5. While the displacement at ultimate load for all conventional joints has approximate similar values that was 17.54, 17.10, 17.74 and 17.49mm.

Beam shear strengths for specimens SE450-W1.5 and SE600-W2.0 were 115.1 (+1.2%) and 151.58 kN (-1.5%) that are close to shear strengths of conventional joints with same width SE450-W1.0 and SE600-W2.0 respectively. While displacement at ultimate load for these wide joints was greater than those of the corresponding conventional joints by 19% and 17% respectively.

However, specimen SE750-W2.5 exhibited a beam shear strength of 162.08 kN, which was approximately 15.7% lower than that of the conventional joint with same beam width, SE750-W1.0.

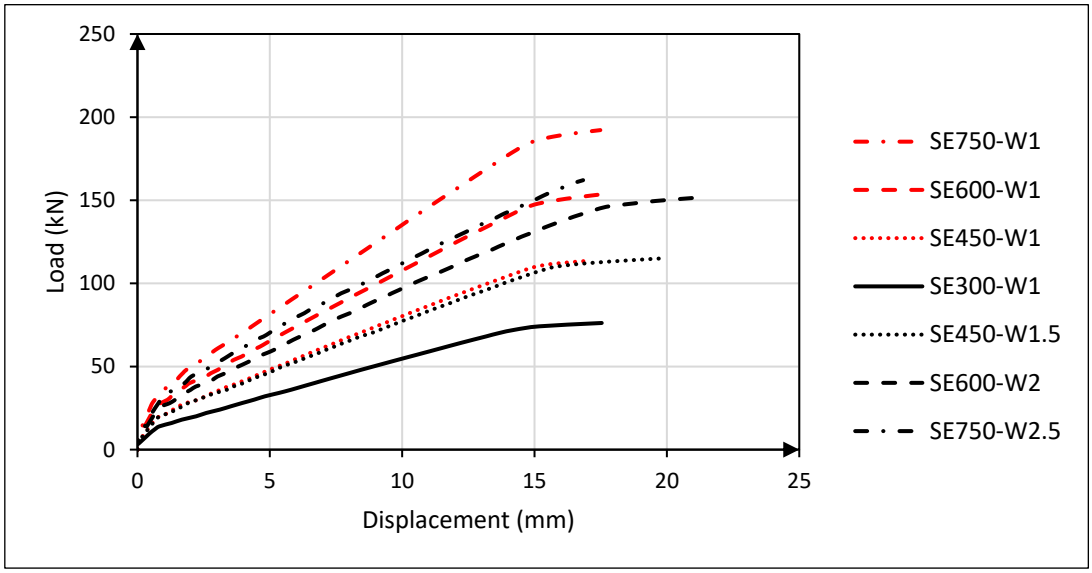

Fig. 9. Load displacement curve for conventional and wide beam column joints with different beam widths

Table 8. Results of load and displacement at first crack and ultimate case for tested joints.

Specimen	First crack		Ultimate		Stiffness (kN/mm)		Ductility	Energy absorption (Joule)
	Load (kN)	Displacement (mm)	Load (kN)	Displacement (mm)	Initial	Post		
SE300-W1.0	22.89	2.81	76.18	17.54	8.14	3.62	6.24	807.36
SE450-W1.0	35.89	3.12	113.68	17.10	10.10	4.73	5.11	1394.52
SE600-W1.0	51.90	3.45	153.94	17.74	12.54	5.81	4.95	1929.55
SE750-W1.0	65.30	3.47	192.19	17.49	15.33	7.82	4.15	1506.80
SE450-W1.5	39.36	3.90	115.10	19.89	11.49	5.57	5.47	1133.00
SE600-W2.0	53.54	4.27	151.58	21.15	15.06	7.14	5.15	1612.32
SE750-W2.5	62.18	4.06	162.08	16.83	18.82	9.05	5.04	1970.51

Concrete and longitudinal beam rebar stresses. In all conventional joint specimens, as well as specimens SE450-W1.5 and SE600-W2, the longitudinal beam reinforcement bars reached their full yield stress of 500 MPa, as shown in (Fig. 10). However, for specimen SE750-W2.5, the beam longitudinal reinforcement bars anchored to column core also reached their full yield stress while rebars, not anchored to column core, reached a maximum stress of only 455 MPa, corresponding to 91% of the yield stress.

Regarding concrete von Mises stresses, the conventional joint specimens, along with SE450-W1.5 and SE600-W2, experienced failure at stresses close to the maximum compressive strength of 30 MPa. The concrete in specimen SE750-W2.5 did not reach its compressive strength capacity. This corresponded to the performance of the beam reinforcement, which did not achieve yield stress. The failure of SE750-W2.5 occurred at a concrete stress of 27.3 MPa, which is 91% of the maximum compressive strength, as shown in (Fig. 11).

Comparing results with ACI 318-19 predictions shows that, joints the conventional joint specimens, along with SE450-W1.5 and SE600-W2 reached their full beam strength capacity while specimen SE750-W2.5 failed due to load represents 91% of its full capacity as shown in *Table 7*.

(Fig. 12) shows joint shear stress distribution on horizontal plane XZ within the joint. It resulted from top longitudinal rebars tension and column shear force as per **eq**. **(5)** It can be noted that shear stress is concentrated at joint region and increases with the increase of beam to column width ratio. As indicated by (Fig. 12) and *Table 7*, specimens with beam to column width ratios of 1 and 1.5 have a

joint shear force approximately 50% and 75%, respectively, of the allowable limit depending on ACI 318-19 provision. Specimen with a ratio of 2 has a joint shear force matches the allowable value while the specimen with a ratio of 2.5 has a joint shear force exceeding the allowable limit by 12%.

By comparing joint shear forces obtained from analytical results ($V_{J,ana}$) and those expected from ACI318-19 ($V_{J,ACI}$), it is revealed that the analytical values are approximately 78% of the ACI predictions as shown in *Table 7*. This indicates that ACI318-19 is slightly conservative in its calculation while the expected joint shear force may be reduced by ratio 20% approximately or the effective joint width could be increased.

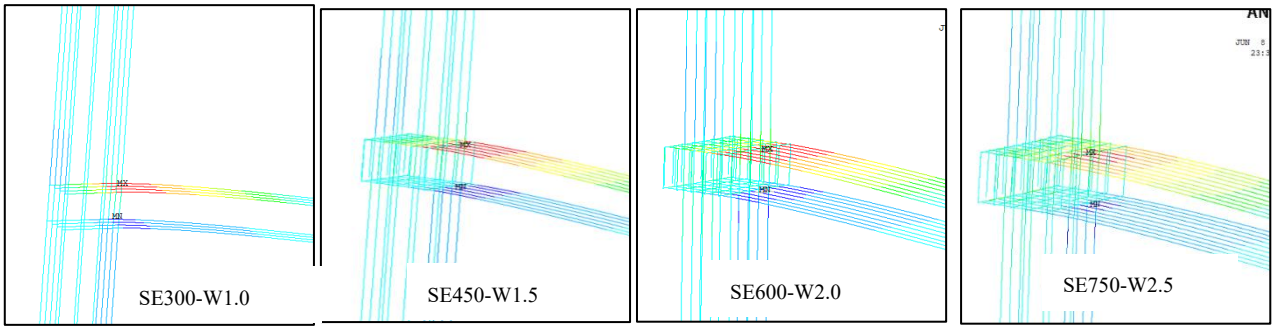

Fig. 10, Longitudinal beam rebar stress for conventional beam column joints and wide beam column joints with different beam to column width ratios**.**

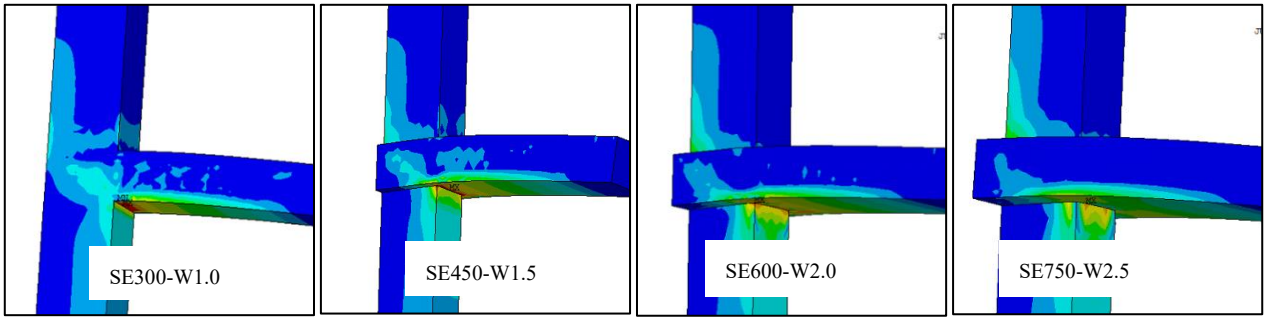

Fig. 11. Von misses concrete stress for conventional beam column joints and wide beam column joints with different beam to column width ratios.

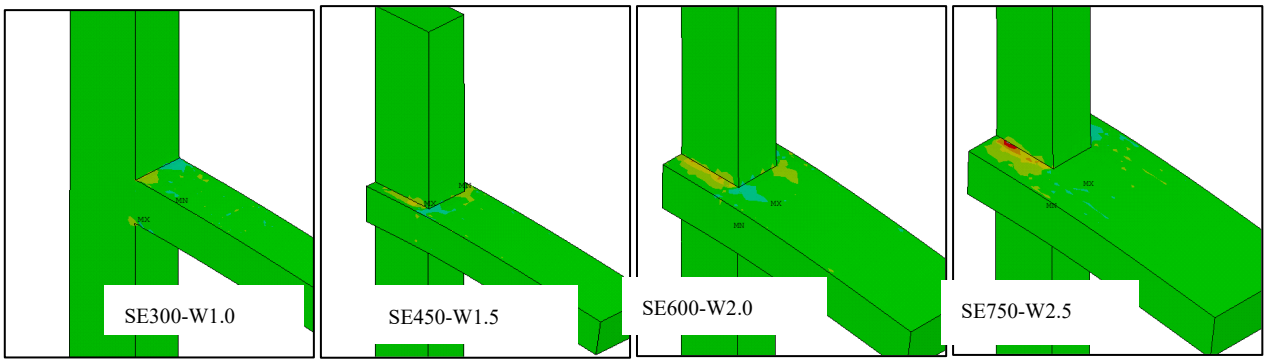

Fig. 12. XZ concrete shear stress for conventional beam column joints and wide beam column joints with different beam to column width ratios.

Ductility, stiffness and energy absorption. The ability of structure or material to deform without damage is called ductility. Ductility index (μ) is defined as ratio between ultimate displacement and yield displacement, and it is used to express the ductility of structure. Ultimate displacement (Δ_u) can be determined easily on load displacement curve while there is difficulty to determine yield displacement (Δ_y) because yield point is not clear on the curve. M.H. El Fakhrany, et al. (2024) [20] suggested a method to determine yield point by drawing a line tangent to the start of the curve and another line tangent to the curve at failure load as shown in (Fig. 13), the two lines intersect at yield displacement. The force corresponding to this displacement on the curve represents yield force.

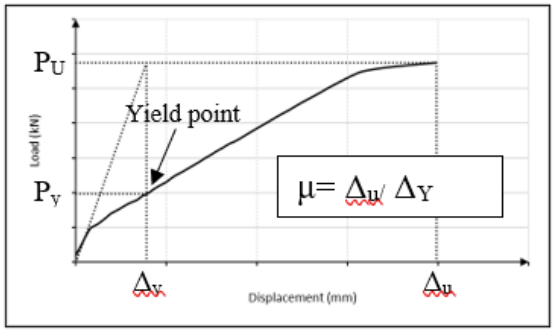

Fig. 13. Determination of ductility index from load displacement curve

For either wide or conventional beam column joints, it can be noted that ductility decreases with the increase of beam width due to stiffness increase.

For conventional joints, ductility decreases by ratios of 13%, 18% and 19% corresponds to beam width increase by 50%, 100% and 150% respectively relative to SE300-W1.

For the same beam width, wide joints have ductility index less than conventional joints by 7%, 4% and 18% for beam widths 450, 600 and 750 mm respectively as shown in (Fig. 14). The loss of ductility for wide beam is expected to be due to load transfer mechanism that depends on shear force and torsional moment through spandrel beam. High loss of ductility of SE750-W2.5 is due to joint shear stress exceeding the allowable limit.

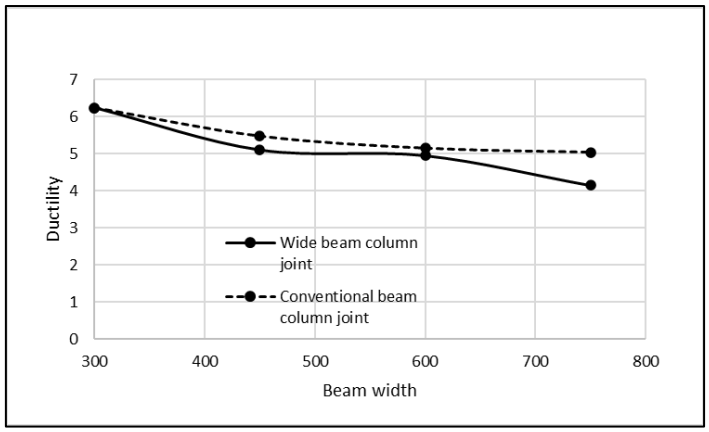

Fig. 14. Effect of beam width on displacement ductility for wide and conventional beam column joints.

Stiffness is the ability of structure to resist deformation where initial stiffness can be measured as the ratio of yield force (P_y) to the yield displacement (Δ_y) while post cracking stiffness can be calculated as the ratio between increase of load to displacement from yield point to ultimate point. (Fig. 15) and **(**Fig. 16**)** clarify the effect of beam width on initial and post cracking stiffness for wide and conventional joints respectively.

For all tested specimens, joint stiffness increases with the increase of beam width. For conventional joints stiffness increased by ratios 1.41, 1.85 and 2.3 for beam width increase by ratios 1.5, 2 and 2.5 relative to SE300-W1.

Also, for the same beam width, conventional joints have more stiffness than corresponding wide beam column joint with ratios of 14%, 20% and 23% for beam to column width ratios 1.5,2 and 2.5 respectively. The loss of stiffness for wide joints is expected to be due to partial force transfer from rebars not anchored to column core. Loss of stiffness causes more beam tip displacement than conventional joints which can be seen in (Fig. 9).

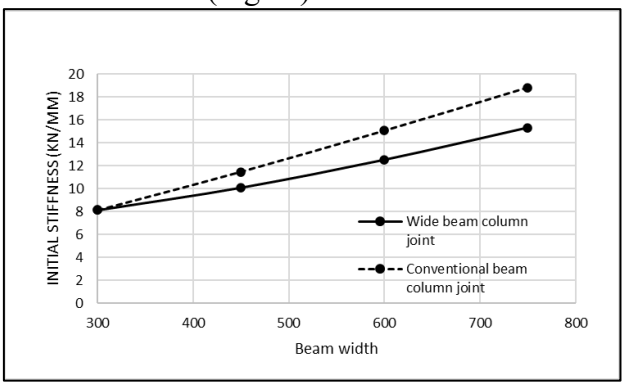

Fig. 15. Effect of beam width on initial stiffness for wide and conventional beam column joints.

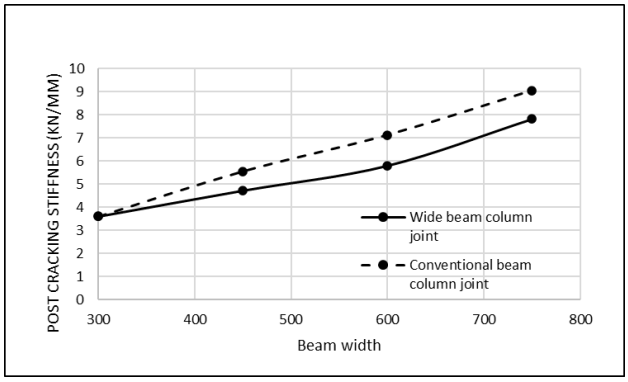

Fig. 16. Effect of width on post cracking stiffness for wide and conventional beam column beam joints.

Energy dissipation is measured from the area under load displacement curve from yield to ultimate so it will be increased by the increase of either of ultimate load or displacement. (Fig. 17) clarifies the effect of beam width on energy dissipation for wide and conventional joints.

It can be noted that conventional joint's ability to dissipate energy increases with the increase of beam width due to increase of beam ultimate load. Energy dissipation increased with ratios of 1.4, 2 and 2.44 aligning with beam width increase ratios of 1.5, 2 and 2.5 compared to SE300-W1.

While wide joint's ability to dissipate energy increases until beam to column width ratio reaches 2 then it decreases with the increase of beam to column width ratio due to the decrease of beam tip displacement for ratios greater than 2.

Also, by comparing wide and conventional joint behavior, it is noted that wide joints dissipate energy more than corresponding conventional joints due to the increase of ultimate displacement until beam to column width ratio of 2. For beam to column width ratio 1.5 and 2, wide joints dissipate energy 1.23 and 1.2 times of corresponding conventional joint. For beam to column width ratio of 2.5, energy dissipation is less than conventional joint by 24%. The loss of energy dissipation is expected to be due to a change of failure mode as this joint with ratio 2.5 failed due to shear.

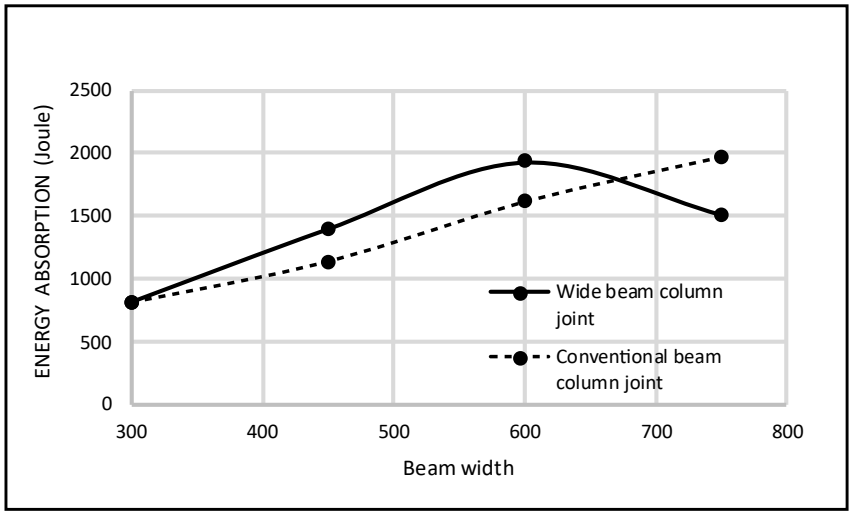

Fig. 17. Effect of beam width on energy absorption for wide and conventional beam column joints.

Conclusions

This paper discusses extensively the behavior of beam column joints. The main parameter studied is beam width for conventional beam column joint and beam to column width ratio for exterior wide beam column joint. The validation with the ACI318-19 provisions is discussed. the main conclusions can be drawn as:

1. Analytical models using ANSYS software are in good convergence to present the deformation, reinforcement strain and the failure modes of exterior beam column joints. The results showed a high correlation between experimental and numerical findings, with accuracy equals 97%.
2. The results for conventional beam-column joints indicated that increasing the beam width led to higher beam shear forces, with conventional joints achieving greater strength and stiffness compared to wide beam-column joints. Additionally, conventional joints showed a higher capacity for energy dissipation, particularly as the beam width increased. However, despite their strength, conventional joints reached their load capacity at lower displacements than wide beam-column joints, which means they exhibited reduced ductility.
3. Increasing the beam-to-column width ratio led to higher beam shear forces, but the increase was more significant at lower width ratios (1 to 1.5). Beyond a width ratio of 2, the increase in strength was minimal, and ductility decreased, especially for wider beams.
4. Ductility decreased as beam width increased, with wide beam-column joints exhibiting lower ductility compared to conventional joints. Stiffness also increased with beam width but was higher in conventional joints than in wide joints.
5. Wide beam-column joints dissipated less energy at beam-to-column width ratios greater than 2, showing that these joints become less effective in energy absorption at wider widths.
6. Most exterior beam column joints failed due to flexure except for wider beams (e.g., SE750-W2.5), which failed due to joint shear and torsion in the spandrel beam. The findings highlighted the need for design improvements to increase joint shear capacity, particularly in wide beam-column joints.
7. A comparison between ACI 318-19 provisions and the analytical results showed that the predicted joint shear capacity based on ACI 318-19 was slightly conservative. The analytical results indicated that the joints generally exceeded the nominal shear strength predicted by the code. For certain specimens, such as those with higher beam-to-column width ratios, the joints failed due to shear and torsional forces, which aligned with the ACI 318-19 predictions. However, the results

suggest that the allowable joint shear stress could be increased by approximately 80% or the effective joint width should be modified to better align with the actual performance observed in the analysis.

References

1. S. S. Mahini and H. R. Ronagh, "A NEW METHOD FOR IMPROVING DUCTILITY IN EXISTING RC ORDINARY MOMENT RESISTING FRAMES USING FRPS," 2007. [Online]. Available: www.SID.ir
2. M. Elsouri and M. H. Harajli, "Seismic response of exterior RC wide beam-narrow column joints: Earthquake-resistant versus as-built joints," *Eng Struct*, vol. 57, pp. 394–405, Dec. 2013, doi: 10.1016/j.engstruct.2013.09.032.
3. S. Mirzabagheri and A. A. Tasnimi, "Reinforced concrete roof exterior wide and conventional beam-column joints under lateral load," *Structural Design of Tall and Special Buildings*, vol. 25, no. 9, pp. 397–411, Jun. 2016, doi: 10.1002/tal.1264.
4. H. Behnam, J. S. Kuang, K. Abdouka, and H. Kong, "BEHAVIOUR OF RC SPANDREL BEAM IN EXTERIOR WIDE BEAM-COLUMN CONNECTIONS," 2016.
5. H. Behnam, J. S. Kuang, and R. Y. C. Huang, "Exterior RC wide beam-column connections: Effect of beam width ratio on seismic behaviour," *Eng Struct*, vol. 147, pp. 27–44, Sep. 2017, doi: 10.1016/j.engstruct.2017.05.044.
6. H. Behnam, J. S. Kuang, and B. Samali, "Parametric finite element analysis of RC wide beam-column connections," *Comput Struct*, vol. 205, pp. 28–44, Aug. 2018, doi: 10.1016/j.compstruc.2018.04.004.
7. H. Behnam, J. S. Kuang, H. F. Wong, Q. Huang, and R. Al-Mahaidi, "Analysis of laterally loaded exterior wide Beam-column connections," *Magazine of Concrete Research*, vol. 70, no. 10, pp. 500–511, May 2018, doi: 10.1680/jmacr.17.00255.
8. H. Behnam, J. S. Kuang, and K. Abdouka, "Effect of post-tensioned spandrel beam on wide beam-column connections," *Magazine of Concrete Research*, vol. 70, no. 1, pp. 28–41, Jan. 2018, doi: 10.1680/jmacr.17.00071.
9. R. P. Bohara, G. Tanapornraweekit, and S. Tangtermsirikul, "Seismic behavior of post-tensioned precast wide U beam–column interior joint: a finite element study," *Asian Journal of Civil Engineering*, vol. 20, no. 4, pp. 603–617, Jun. 2019, doi: 10.1007/s42107-019-00129-x.
10. X. Gao, D. Xiang, Y. He, and J. Li, "Shear Deformation and Force Transfer of Exterior Beam- Column Joints," *ACI Struct J*, vol. 117, no. 6, Nov. 2020, doi: 10.14359/51728074.
11. V. V S and N. Mohan, "Exterior Type-2 Wide Beam - Column Connection an Overview," 2020. [Online]. Available: http://www.ijser.org
12. Pakzad and M. Khanmohammadi, "Experimental cyclic behavior of code-conforming exterior wide beam-column connections," *Eng Struct*, vol. 214, Jul. 2020, doi: 10.1016/j.engstruct.2020.110613.
13. R. Y. C. Huang and J. S. Kuang, "Predicting Strength of Exterior Wide Beam–Column Joints for Seismic Resistance," *Journal of Structural Engineering*, vol. 146, no. 2, Feb. 2020, doi: 10.1061/(asce)st.1943-541x.0002488.
14. R. P. Bohara, G. Tanapornraweekit, and S. Tangtermsirikul, "Experimental and numerical investigation on seismic performance of a composite wide beam-column interior joint," *Structures*, vol. 30, pp. 560–573, Apr. 2021, doi: 10.1016/j.istruc.2021.01.033.
15. J. H. Kim, S.-H. Choi, S.-J. Han, H. Jeong, J.-Y. Lee, and K. S. Kim, "Effect of reinforcing details on seismic behavior of RC exterior wide beam-column joint," *Earthquakes and Structures*, vol. 25, no. 4, pp. 283–296, Oct. 2023.
16. Q. Jiang, W. Su, Y. Feng, J. Shen, Y. Fan, and D. Xuan, "Seismic performance of <scp>RC</scp> exterior wide beam–column joints," *Structural Concrete*, vol. 25, no. 6, pp. 5037–5055, Dec. 2024, doi: 10.1002/suco.202300830.
17. S. S. Mahini and H. R. Ronagh, "A New Method for Improving Ductility In Existing RC Ordinary Moment Resisting Frames Using FRPs," 2007. [Online]. Available: www.SID.ir
18. "Building code requirements for structural concrete (ACI 318-19) commentary on building code requirements for structural concrete (ACI 318R-19)", Available From: www.amiralikhalvati.com
19. ACI 352R-02. 2002. Recommendations for design of beam-column connections in monolithic reinforced concrete structures, American Concrete Institute, Farmington Hills, Michigan.
20. M. H. El Fakhrany, A. el-Zamrawi, W. Ibrahim, and A. Sherif, "Flexural performance of rapid-hardening concrete (RHC) beams with tension lap splice," *Beni Suef Univ J Basic Appl Sci*, vol. 13, no. 1, Dec. 2024, doi: 10.1186/s43088-024-00478-w.